PERGAMON

International Journal of Solids and Structures 39 (2002) 1575–1590

INTERNATIONAL JOURNAL OF SOLIDS and STRUCTURES

www.elsevier.com/locate/ijsolstr

Interaction among interface, multiple cracks and dislocations

Xueli Han, Fernand Ellyin *, Zihui Xia

Department of Mechanical Engineering, University of Alberta, Edmonton, Alberta, T6G 2G8 Canada

Received 19 December 2000; received in revised form 1 November 2001

Abstract

The interaction problem of a number of arbitrary oriented and distributed cracks and/or dislocations in bonded bi-material half planes, are considered in a unified method. The basic solution of a single dislocation in a bonded half plane and the superposition technique, are used. The method has high accuracy and computational efficiency. It can treat the combined interaction of cracks, dislocations and interface. Several examples are given to show certain interaction effects, especially among cracks near an interface. © 2002 Elsevier Science Ltd. All rights reserved.

Keywords: Bonded planes; Crack growth; Energy release rate; Interaction among cracks; Interface crack

1. Introduction

Interfaces, imperfections (such as dislocations and cracks) and their interactions play an important role in understanding the fracture behavior of multiphase solids, and have received considerable attention. This study was mainly motivated by the fact that damage development in composite materials is characterized by the initiation and accumulation of multiple, interacting cracks. This multiplicity of interacting and competing modes is in contrast to the interaction and self-similar propagation of a singular crack observed in isotropic, homogeneous materials. For homogeneous materials, interactions among multiple cracks, or between a crack and dislocation, have been analyzed by a number of investigators, and they will not be mentioned here. For inhomogeneous materials, interactions of cracks, dislocations and interfaces, have also been considered by several researchers. Among them, Chen (1986), Isida and Noguchi (1993), Hu et al. (1994), and Otsu et al. (1999) have provided solution for cracks interacting in bonded planes, but excluding interface cracks. Using complex potential method, Suo (1989) and Zhang and Li (1992) have analyzed the problem of a dislocation interacting with an interfacial crack. Employing displacement dislocations method in conjunction with Mellin transforms, Goree and Venezia (1977) investigated the problem of an interface crack with a perpendicular crack. Combining pseudo-traction and dislocation method, Zhao and Chen (1996) considered the interaction problems of an interface crack with a parallel sub-interface crack. Based on the solution of a concentrated body force in bonded half planes with an interface crack, Isida and Noguchi (1994) investigated the problem of non-interface crack(s) interacting with an interfacial one. In the

* Corresponding author. Tel.: +1-780-492-2009; fax: +1-780-492-2200.
E-mail address: fernand.ellyin@ualberta.ca (F. Ellyin).

PII: S0020-7683(01)00274-8

works cited above, interfacial cracks are either excluded or limited to a single one only. There are still some interaction problems of cracks in bonded dissimilar media, especially associated ones with more than one interface crack (interacting with other cracks and dislocations), which have not yet been solved.

For the interacting elastic problem of multiple cracks, except for numerical approaches such as finite element or boundary element method, the usual analytical–numerical approach is superposition technique which uses some kind of basic solutions. For example in the body force method (or "pseudo-traction" method or distributed dislocation method), the elastic solution of (arbitrary) distributed body forces (tractions or dislocations) applied along a single crack is the basic which is required, and their density is determined from the boundary conditions. Ample references are provided regarding different methods used for multiple cracks in an article by Burton and Phoenix (2000). With respect to the superposition technique and corresponding body force method, the interested readers are encouraged to consult works by Isida and Noguchi (1993, 1994), in the case of "pseudo-tractions" method, that by Kachanov (1994), and for the distributed dislocation method, the monograph by Hills et al. (1996), among others.

In this paper we will use a unified technique to analyze the interaction problems among arbitrarily oriented and distributed cracks and dislocations, including interfacial ones, in bonded dissimilar half planes. The fundamental solution is that of a dislocation in a bonded half planes, and the superposition technique and the complex potential method will be used. The method presented here is a simple one yet versatile enough to solve interaction problems among interfacial cracks, non-interface cracks and dislocations. In this new method, there are no limits to the number, orientations and location of cracks and dislocations.

2. Formulation

2.1. Problem statement

Let us consider two bonded half planes with multiple interfacial cracks and/or dislocations, and other arbitrarily oriented and distributed cracks and/or dislocations, see Fig. 1. A global coordinate system Oxy is chosen with the x-axis coinciding with the bi-material interface. Material 1 occupies the upper half plane denoted by the domain D_1, and material 2 occupies the lower half planes D_2. The Young's moduli, shear moduli and Poisson's ratios are denoted by E_1, μ_1, v_1, and E_2, μ_2, v_2, respectively. It is assumed that M edge dislocations and N cracks are scattered on the plane. We concentrate on the mth dislocation and jth crack, and consider a local tangential–normal coordinate system $O_j x_j y_j$ associated with the jth crack. The half length, inclination angle, and position vector of the center O_j of the jth crack are denoted by a_j, θ_j and z_{O_j}, respectively.

Let the solid be subjected to far field stresses denoted by σ_{x1}^{∞} (in D_1), σ_{x2}^{∞} (in D_2), σ_y^{∞} and σ_{xy}^{∞}. The applied stresses in the x-direction are related such that to produce constant strains in the x-direction at points remote from the crack. The following relation must then hold (see e.g. Goree and Venezia (1977) and Isida and Noguchi (1993)):

$$\sigma_{x1}^{\infty} = \frac{1}{1+\kappa_1}\left\{\frac{\mu_1}{\mu_2}(1+\kappa_2)\sigma_{x2}^{\infty} + \left[3-\kappa_1-\frac{\mu_1}{\mu_2}(3-\kappa_2)\right]\sigma_y^{\infty}\right\} \tag{1}$$

with $\kappa_i = 3-4v_i$ for plane strain and $\kappa_i = (3-v_i)/(1+v_i)$ for plane stress, $i = 1, 2$.

The interaction among dislocations and cracks in bonded half planes can be obtained by the superposition technique. The M dislocations and N cracks system is divided into M single-dislocation and N single-crack problems. Cracks can be modeled by continuously distributed dislocations. Based on the superposition technique, the solutions of a single dislocation and a single crack in a bonded half planes are

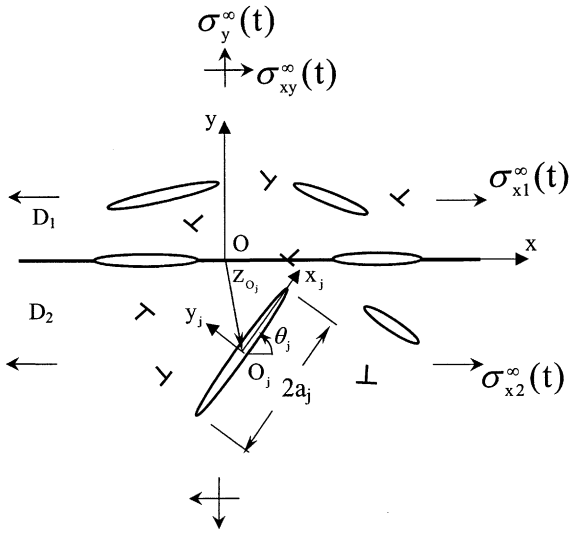

Fig. 1. Bonded half planes with arbitrarily distributed cracks and dislocations.

required for the current analysis. The single crack solution can also be derived from the single dislocation solution, so the fundamental single dislocation solution is given first in details.

2.2. Basic formulae and fundamental solution

For an isotropic elastic body under plane deformation, the stress components can be represented by two complex potentials $\Phi(z)$ and $\Omega(z)$ (see e.g. Muskhelishvili (1953) and Suo (1989)), as

$$\begin{aligned}\sigma_{xx}+\sigma_{yy}&=2[\Phi(z)+\overline{\Phi(z)}]\\ \sigma_{yy}-\mathrm{i}\sigma_{xy}&=\Phi(z)+\overline{\Omega(z)}+(z-\bar{z})\overline{\Phi'(z)}\end{aligned} \tag{2}$$

where a bar over a symbol indicates the conjugate form.

For a single edge dislocation located at $z=s_m$ in D_2 (one domain of bonded half planes), the complex potentials was given by Suo (1989) as,

$$\Phi(z)=\begin{cases}(1+\Lambda)\Phi_0(z), & z \text{ in } D_1\\ \Phi_0(z)+\Pi\overline{\Omega_0}(z), & z \text{ in } D_2\end{cases}\quad \Omega(z)=\begin{cases}(1+\Pi)\Omega_0(z), & z \text{ in } D_1\\ \Omega_0(z)+\Lambda\overline{\Phi_0}(z), & z \text{ in } D_2\end{cases} \tag{3a}$$

where

$$\Phi_0(z)=B_m\frac{1}{z-s_m},\quad \Omega_0(z)=\overline{B}_m\frac{1}{z-s_m}+B_m\frac{\bar{s}_m-s_m}{(z-s_m)^2},\quad B_m=\frac{\mu_2}{\mathrm{i}\pi(\kappa_2+1)}(b_{mx}+\mathrm{i}b_{my}) \tag{3b}$$

and b_{mx} and b_{my} are the x- and y-components of the Burger's vector of the dislocation. Here Λ and Π measure the inhomogeneity by

$$\Lambda=\frac{\alpha+\beta}{1-\beta},\quad \Pi=\frac{\alpha-\beta}{1+\beta} \tag{3c}$$

with α and β being Dundurs' parameters,

$$\alpha = \frac{\mu_1(\kappa_2+1)-\mu_2(\kappa_1+1)}{\mu_1(\kappa_2+1)+\mu_2(\kappa_1+1)}, \quad \beta = \frac{\mu_1(\kappa_2-1)-\mu_2(\kappa_1-1)}{\mu_1(\kappa_2+1)+\mu_2(\kappa_1+1)} \tag{3d}$$

Substituting Eq. (3a) into Eq. (2), the field induced by the dislocation can be calculated. In particular, the stress components (in the local coordinate system $O_k x_k y_k$) at a point z ($= z_{O_k} + x_k e^{i\theta_k}$) along the kth crack line (with angle θ_k), can be obtained as

$$\sigma_{y_k y_k} + i\sigma_{x_k y_k} = B_m g_1(z, s_m) + \overline{B}_m g_2(z, s_m) \tag{4}$$

where

$$\begin{aligned} g_1 &= \frac{1}{z-s_m} - e^{2i\theta_k}\frac{\bar{z}-\bar{s}_m}{(z-s_m)^2} + \Pi\left[\frac{1}{z-\bar{s}_m} + \frac{\bar{s}_m - s_m}{(\bar{z}-s_m)^2} - e^{2i\theta_k}\frac{\bar{z}-\bar{s}_m}{(z-\bar{s}_m)^2}\right] \\ g_2 &= \frac{1}{\bar{z}-\bar{s}_m} + e^{2i\theta_k}\frac{1}{z-s_m} + \Pi\left[\frac{1}{\bar{z}-s_m} + \frac{s_m-\bar{s}_m}{(z-\bar{s}_m)^2} + e^{2i\theta_k}\frac{(s_m-\bar{s}_m)(z+\bar{s}_m-2\bar{z})}{(z-\bar{s}_m)^3}\right] + \Lambda e^{2i\theta_k}\frac{1}{z-\bar{s}_m} \end{aligned} \tag{5a}$$

if the kth crack is also located in the same domain D_2 with the mth dislocation or is on the interface. However, if the kth crack is located in D_1, a different domain than the mth dislocation, then

$$\begin{aligned} g_1 &= (1+\Lambda)\frac{1}{z-s_m} + e^{2i\theta_k}\frac{(1+\Pi)(\bar{s}_m-s_m)-(1+\Lambda)(\bar{z}-s_m)}{(z-s_m)^2} \\ g_2 &= (1+\Lambda)\frac{1}{\bar{z}-\bar{s}_m} + e^{2i\theta_k}(1+\Pi)\frac{1}{z-s_m} \end{aligned} \tag{5b}$$

Similarly, when the edge dislocation is located at $z = s_m$ in domain D_1, the results can be obtained by simply exchanging the subscripts 1 and 2 in Eqs. (3a), (3b) and (3d), respectively. For the sake of brevity, in the following, the effects of a dislocation or a crack in the domain D_1 on other dislocations or cracks will not be repeated. However, the numerical examples will contain this case.

The solution of an interfacial dislocation can be obtained as the dislocation approaches the interface from any domain, such as D_2 of bonded half planes. When the dislocation is located at the interface $z = s_m$, noting that s_m is real, its complex potentials are obtained from Eq. (3a) as,

$$\Phi(z) = \begin{cases} (1+\Lambda)\Phi_0(z), & z \text{ in } D_1 \\ (1+\Pi)\Phi_0(z), & z \text{ in } D_2 \end{cases} \quad \Omega(z) = \begin{cases} (1+\Pi)\Omega_0(z), & z \text{ in } D_1 \\ (1+\Lambda)\Omega_0(z), & z \text{ in } D_2 \end{cases} \tag{6}$$

with

$$\Phi_0(z) = B_m\frac{1}{z-s_m}, \quad \Omega_0(z) = \overline{B}_m\frac{1}{z-s_m}, \quad B_m = \frac{\mu_2}{i\pi(\kappa_2+1)}(b_{mx}+ib_{my})$$

The stress components along the kth crack line, induced by the interface dislocation, can be obtained and expressed in the form of Eq. (4), with

$$g_1 = (1+\Pi)\frac{1}{z-s_m} - e^{2i\theta_k}(1+\Pi)\frac{\bar{z}-s_m}{(z-s_m)^2}, \quad g_2 = (1+\Pi)\frac{1}{\bar{z}-s_m} + e^{2i\theta_k}(1+\Lambda)\frac{1}{z-s_m} \tag{7a}$$

if the kth crack is also located in the domain D_2. However, if the kth crack is located in the domain D_1, then

$$g_1 = (1+\Lambda)\frac{1}{z-s_m} - e^{2i\theta_k}(1+\Lambda)\frac{\bar{z}-s_m}{(z-s_m)^2}, \quad g_2 = (1+\Lambda)\frac{1}{\bar{z}-s_m} + e^{2i\theta_k}(1+\Pi)\frac{1}{z-s_m} \tag{7b}$$

Finally, if the kth crack is on the interface

$$g_1 = 0, \quad g_2 = (2 + \Pi + \Lambda)\frac{1}{x - s_m} + (\Lambda - \Pi)\mathrm{i}\pi\delta(x - s_m) \tag{7c}$$

where δ denotes the Dirac delta function.

Up to this point, the complex functions for an edge dislocation in bonded half planes have been given irrespective of the position of dislocation, be it either in a half plane or in the interface. Thus the stress field along any crack line (for an arbitrarily located crack) produced by the dislocation, are now known.

2.3. Solution of a crack in a bonded half planes

A crack can be modelled by continuously distributed edge dislocations along the crack line where the dislocation density function is determined from boundary conditions. Since the solution of a single dislocation is known, the crack field due to the continuously distributed dislocations can be derived by integrating the effect of a single dislocation.

The stress components along the kth crack line, induced by the jth crack with dislocation density function $B_j(\xi_j)$ ($|\xi_j| < a_j$), are obtained by integrating the single dislocation result as

$$\sigma_{y_k y_k} + \mathrm{i}\sigma_{x_k y_k} = \int_{-a_j}^{a_j} [B_j(\xi_j) g_1(x_k, \xi_j) + \overline{B}_j(\xi_j) g_2(x_k, \xi_j)]\,\mathrm{d}\xi_j \tag{8}$$

where x_k and ξ_j are the coordinates of the point z (on the kth crack line) and s_j (on the jth crack line), i.e. $z = z_{O_k} + x_k \mathrm{e}^{\mathrm{i}\theta_k}$, $s_j = z_{O_j} + \xi_j \mathrm{e}^{\mathrm{i}\theta_j}$, and $g_i(z, s_j) = g_i(z_{O_k} + x_k \mathrm{e}^{\mathrm{i}\theta_k}, z_{O_j} + \xi_j \mathrm{e}^{\mathrm{i}\theta_j})$ will be denoted simply by $g_i(x_k, \xi_j)$ ($i = 1, 2$), and the functions $g_i(z, s_j)$ for a single dislocation located in s_j are known from the previous section. As a particular case, for the integration along kth crack line itself, the corresponding $g_i(z, s_j)$ can be simplified from Eq. (5a) as

$$\begin{aligned} g_1 &= \Pi\left[\frac{1}{z - \bar{s}_k} + \frac{\bar{s}_k - s_k}{(\bar{z} - s_k)^2} - \mathrm{e}^{2\mathrm{i}\theta_k}\frac{\bar{z} - \bar{s}_k}{(z - \bar{s}_k)^2}\right] \\ g_2 &= 2\mathrm{e}^{2\mathrm{i}\theta_k}\frac{1}{z - s_k} + \Pi\left[\frac{1}{\bar{z} - s_k} + \frac{s_k - \bar{s}_k}{(z - \bar{s}_k)^2} + \mathrm{e}^{2\mathrm{i}\theta_k}\frac{(s_k - \bar{s}_k)(z + \bar{s}_k - 2\bar{z})}{(z - \bar{s}_k)^3}\right] + \Lambda\mathrm{e}^{2\mathrm{i}\theta_k}\frac{1}{z - \bar{s}_k} \end{aligned} \tag{9a}$$

where $z = z_{O_k} + x_k \mathrm{e}^{\mathrm{i}\theta_k}$, $s_k = z_{O_k} + \xi_k \mathrm{e}^{\mathrm{i}\theta_k}$. When the kth crack is on the interface, g_1 and g_2 can be obtained from Eq. (7c) as

$$g_1 = 0, \quad g_2 = (2 + \Pi + \Lambda)\frac{1}{x_k - \xi_k} + (\Lambda - \Pi)\mathrm{i}\pi\delta(x_k - \xi_k) \tag{9b}$$

Thus, the stress fields along any crack line produced by the distributed dislocations along any (arbitrary) crack line, including itself, are obtained.

2.4. Integral equations

The solutions of a single dislocation and a crack are thus far known. Using the superposition technique, summing the effects of all dislocations and cracks on the presumed location of the kth crack, and imposing the traction-free condition (in the local coordinate system $O_k x_k y_k$), we get

$$\begin{aligned} &\sum_{m=1}^{M}[B_m g_1(z, s_m) + \overline{B}_m g_2(z, s_m)] + \sum_{j=1}^{N}\int_{-a_j}^{a_j}[B_j(\xi_j) g_1(x_k, \xi_j) + \overline{B}_j(\xi_j) g_2(x_k, \xi_j)]\,\mathrm{d}\xi_j + \sigma^0_{y_k y_k} + \mathrm{i}\sigma^0_{x_k y_k} \\ &\quad = 0 \quad k = 1, \ldots, N \end{aligned} \tag{10}$$

where $z = z_{O_k} + x_k e^{i\theta_k}$ is on the kth crack line. Note that $\sigma^0_{y_k y_k}$ and $\sigma^0_{x_k y_k}$ are the stress components at the location of the kth crack produced by external loads, excluding all dislocations and cracks. They are determined from

$$\sigma^0_{y_k y_k} + i\sigma^0_{x_k y_k} = \frac{1}{2}(\sigma^\infty_x + \sigma^\infty_y)(1 - e^{2i\theta_k}) + (\sigma^\infty_y + i\sigma^\infty_{xy})e^{2i\theta_k}$$

with $\sigma^\infty_x = \sigma^\infty_{x1}$ and σ^∞_{x2} for the crack in domain D_1 and D_2, respectively, and $\sigma^0_{y_k y_k} + i\sigma^0_{x_k y_k} = \sigma^\infty_y + i\sigma^\infty_{xy}$ for the crack in the interface. In the governing equations (10), the dislocation density functions $B_j(\xi_j)$ $(j = 1, \ldots, N)$ are unknown and hence have to be determined.

Assuming there are N_1 non-interfacial cracks $(k = 1, \ldots, N_1)$ and N_2 $(= N - N_1)$ interfacial ones $(k = N_1 + 1, \ldots, N)$, and depending on the characteristic of the integral kernels, Eq. (10) can be expressed explicitly in terms of singular integral equations as follows,

$$2e^{i\theta_k}\int_{-a_k}^{a_k}\frac{\overline{B}_k(\xi_k)}{x_k - \xi_k}\,d\xi_k + \int_{-a_k}^{a_k}\left\{B_k(\xi_k)g_1(x_k,\xi_k) + \overline{B}_k(\xi_k)\left[g_2(x_k,\xi_k) - 2e^{i\theta_k}\frac{1}{x_k - \xi_k}\right]\right\}d\xi_k + \sum_{j=1, j\neq k}^{N}\int_{-a_j}^{a_j}[B_j(\xi_j)g_1(x_k,\xi_j) + \bar{B}_j(\xi_j)g_2(x_k,\xi_j)]\,d\xi_j = -p(x_k), \quad k = 1, \ldots, N_1 \tag{11a}$$

$$(2 + \Pi + \Lambda)\int_{-a_k}^{a_k}\frac{\overline{B}_k(\xi_k)}{x_k - \xi_k}\,d\xi_k + [(\Lambda - \Pi)i\pi\overline{B}_k(x_k)] + \sum_{j=1, j\neq k}^{N}\int_{-a_j}^{a_j}[B_j(\xi_j)g_1(x_k,\xi_j) + \overline{B}_j(\xi_j)g_2(x_k,\xi_j)]\,d\xi_j = -p(x_k), \quad k = N_1 + 1, \ldots, N \tag{11b}$$

with $|x_k| < a_k$, $p(x_k) = \sum_{m=1}^{M}[B_m g_1(z, s_m) + \overline{B}_m g_2(z, s_m)] + (\sigma^0_{y_k y_k} + i\sigma^0_{x_k y_k})$ which are known functions, and $z = z_{O_k} + x_k e^{i\theta_k}$. Therefore, the governing equations for non-interfacial cracks, Eq. (11a), are singular integral equations of the first kind, and for the interfacial cracks, Eq. (11b), the singular integral equations are of the second kind.

In addition, the single-valued condition of displacements results in the following equations (see e.g. Erdogan et al. (1973) and Chen (1995)):

$$\int_{-a_k}^{a_k} B_k(\xi_k)\,d\xi_k = 0, \quad k = 1, \ldots, N \tag{12}$$

Thus, Eqs. (11a) and (11b) along with constraint conditions (12) provide the integral equation representation of interactions in a general bonded half planes system containing M dislocations and N cracks. When the governing integral equations are solved, the dislocation density functions $B_k(\xi_k)$ $(k = 1, \ldots, N)$, for each crack are determined, and the interaction fields are then obtained by summing all the single dislocation and single crack fields.

2.5. Numerical solution procedure

The integral equations (11a) and (11b) can be solved by using polynomial expansion technique (see e.g. Erdogan et al. (1973)). When the cracks are non-interfacial, the dislocation density functions $B_k(\xi_k)$ are expressed by the first kind of Chebyshev polynomials as follows:

$$\overline{B}_k(\xi_k) = \frac{1}{\sqrt{1 - \tau_k^2}}\sum_{l=0}^{\infty} b_{kl}T_l(\tau_k) \tag{13a}$$

where $\tau_k = \xi_k/a_k$, $|\xi_k| < a_k$, $|\tau_k| < 1$, $T_l(\ )$ are the Chebyshev polynomials of the first kind, and b_{kl} are coefficients of the Chebyshev polynomials which have to be determined. For the interfacial cracks, $B_k(\xi_k)$ are expressed by the Jacobi polynomials,

$$\overline{B}_k(\xi_k) = W(\tau_k)\sum_{l=0}^{\infty} b_{kl}P_l^{(\alpha',\beta')}(\tau_k) \tag{13b}$$

where

$$\tau_k = \xi_k/a_k, \quad W(\tau_k) = (1-\tau_k)^{\alpha'}(1+\tau_k)^{\beta'}, \quad \alpha' = -\tfrac{1}{2} + \mathrm{i}\varepsilon, \quad \beta' = -\tfrac{1}{2} - \mathrm{i}\varepsilon, \quad \varepsilon = \frac{1}{2\pi}\ln\frac{1-\beta}{1+\beta}$$

β is one of the Dundurs' parameters, Eq. (3d), $P_l^{(\alpha',\beta')}(\ )$ are the Jacobi polynomials, and b_{kl} are coefficients of the Jacobi polynomials to be determined.

Substituting the polynomial form Eqs. (13a) and (13b) of $B_k(\xi_k)$ into the constraint conditions (12), we get $b_{k0} = 0$ $(k = 1, \ldots, N)$. When Eqs. (13a) and (13b) is substituted into the singular integral equations (11a) and (11b), they reduce to a system of infinite series equations. The system of series equations can be solved by a numerical method, such as the weighted residual method (see e.g. Erdogan et al. (1973)), or by series expansion method (see e.g. Gross (1982)). When the infinite series (13a) and (13b) is truncated at the L_kth term, then the unknown coefficients b_{kl} $(k = 1, \ldots, N,\ l = 1, \ldots, L_k)$ become finite. Here we solve the series equations by the simple collocation method, i.e. each equation is satisfied at some discrete points on the crack location. Thus the series equations are converted into a system of linear algebraic equations which can be solved easily.

Following the solution of governing equations, the dislocation density functions are determined, and the stress and strain at any point of the plane are obtained by superposition. For a crack, the singular stress term at the crack tips is the term resulting from the distributed dislocations along the crack line. The stress components along the crack line (retaining only the singular term) are given by:

$$\sigma_{y_k y_k} + \mathrm{i}\sigma_{x_k y_k} = 2\mathrm{e}^{\mathrm{i}\theta_k}\int_{-a_k}^{a_k}\frac{\overline{B}_k(\xi_k)}{x_k - \xi_k}\,\mathrm{d}\xi_k = 2\mathrm{e}^{\mathrm{i}\theta_k}\pi\sum_l b_{kl}\left(\tau_k - \sqrt{\tau_k^2 - 1}\right)^l \Big/ \sqrt{\tau_k^2 - 1} \tag{14a}$$

if the kth crack is a non-interfacial one, with $\tau_k = \xi_k/a_k$, $|x_k| > a_k, |\tau_k| > 1$. However, if the kth crack is an interfacial one, then

$$\sigma_{y_k y_k} + \mathrm{i}\sigma_{x_k y_k} = (2 + \Pi + \Lambda)\int_{-a_k}^{a_k}\frac{\overline{B}_k(\xi_k)}{x_k - \xi_k}\,\mathrm{d}\xi_k = -(2 + \Pi + \Lambda)\mathrm{i}\pi(1+\beta)w(\tau_k)\sum_l b_{kl}P_l^{(\alpha',\beta')}(\tau_k) \tag{14b}$$

with

$$w(\tau) = \mathrm{i}\sqrt{\frac{1-\beta}{1+\beta}}(\tau-1)^{\alpha'}(\tau+1)^{\beta'} \text{ for } \tau > 1, \text{ and } w(\tau) = -\mathrm{i}\sqrt{\frac{1-\beta}{1+\beta}}(1-\tau)^{\alpha'}(-1-\tau)^{\beta'} \text{ for } \tau < -1$$

The stress intensity factors can thus be obtained as,

$$K_k = K_{k\mathrm{I}} + \mathrm{i}K_{k\mathrm{II}} = \lim_{r\to 0}\sqrt{2\pi r}(\sigma_{y_k y_k} + \mathrm{i}\sigma_{x_k y_k}) = \sqrt{\pi a_k}\left[\pm 2\mathrm{e}^{\mathrm{i}\theta_k}\pi\sum_l b_{kl}T_l(\pm 1)\right] \tag{15a}$$

if the kth crack is non-interfacial one. However, if the kth crack is an interfacial one, then the complex stress intensity factors are given by,

$$K_k = K_{k\mathrm{I}} + \mathrm{i}K_{k\mathrm{II}} = \lim_{r\to 0}\sqrt{2\pi r}\left(\frac{r}{2a_k}\right)^{\mp\mathrm{i}\varepsilon}(\sigma_{y_k y_k} + \mathrm{i}\sigma_{x_k y_k}) = \sqrt{\pi a_k}\left[\pm(2 + \Pi + \Lambda)\pi\sum_l b_{kl}P_l^{(\alpha',\beta')}(\pm 1)\right] \tag{15b}$$

where r is the distance ahead of the crack tips along the crack line, and the quantities with upper and lower signs refer to the right- and left-hand tips of the crack, respectively.

Finally, the energy release rate is determined from,

$$G_k = \frac{1}{E'}|K_k|^2 \tag{16}$$

where $\frac{1}{E'} = \frac{\kappa_1+1}{8\mu_1}$ for the kth crack in the domain D_1, $\frac{1}{E'} = \frac{\kappa_2+1}{8\mu_2}$ for the crack in D_2, and $\frac{1}{E'} = \frac{1-\beta^2}{2}\left(\frac{\kappa_1+1}{8\mu_1} + \frac{\kappa_2+1}{8\mu_2}\right)$ for the crack on the interface.

3. Numerical examples and results

First, the computational accuracy of the present method needs to be checked. There are numerous published works, e.g. see the stress intensity factors handbook by Murakami et al. (1987), in which the results for different crack cases are given. We have compared various results with those of ours (which we will not mention here), and the agreement was found to be very good. In the following, we only show two examples for the sake of comparison. The first one is an interface crack interacting with an edge dislocation, and the second one is an interface crack interacting with another crack.

Fig. 2 shows an interfacial edge dislocation interacting with an interfacial crack. This problem was investigated by Zhang and Li (1992), and analytic formulae of shielded or anti-shielded stress intensity factors were presented. The results of stress intensity factors calculated by the present method are given in Table 1, which are shown to be identical up to the fifth decimal points compared with the analytical results. When the dislocation becomes closer to the crack, to maintain the accuracy of results, the number of series terms (and collocation points) L, has to be increased. However, even for a very close dislocation, the series terms need not be high to obtain a quite accurate result.

Fig. 3 shows an interfacial crack interacting with a parallel sub-interface crack. This problem was investigated by Zhao and Chen (1996). The results of stress intensity factors by the present method are given in Table 2, and compared with those given by Chen and Hasebe (1998). It is seen that the results agree well,

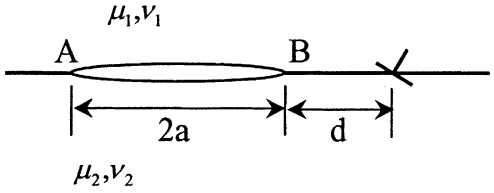

Fig. 2. An interfacial crack interacting with a dislocation.

Table 1
The stress intensity factors (normalized by $\mu_2|b_m|/\sqrt{\pi a}$) at the tips of an interfacial crack, produced by an edge dislocation $b_m = b_1$ in the interface (see Fig. 2), with $\nu_1 = \nu_2 = 0.3$ and in plane stress condition

d/a	L	$\mu_1/\mu_2 = 0.1$		$\mu_1/\mu_2 = 10$	
		K' at A	K' at B	K' at A	K' at B
1.0	11	(−7.6438E−03, −5.4806E−02)	(2.2931E−02, −9.3061E−02)	(7.6438E−02, −0.54806)	(−0.22931, −0.93061)
0.5	14	(−8.6563E−03, −7.1820E−02)	(4.3282E−02, −0.15586)	(8.6563E−02, −0.71820)	(−0.43282, −1.5586)
0.1	30	(−7.9120E−03, −0.10178)	(0.16615, −0.43734)	(7.9120E−02, −1.0178)	(−1.6615, −4.3734)

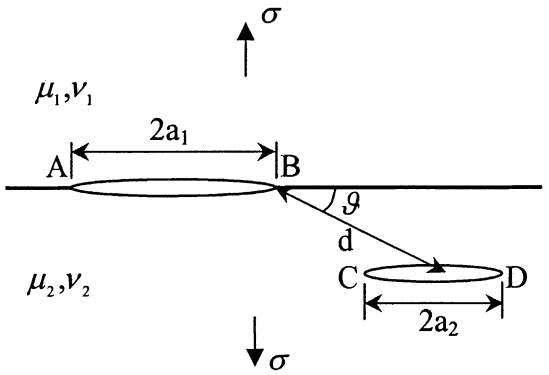

Fig. 3. An interface crack interacting with a parallel sub-interface crack.

Table 2
The stress intensity factors (normalized by $\sigma\sqrt{a_1}$) for an interface crack interaction with a parallel sub-interface crack (see Fig. 3), compared with the results by Chen and Hasebe (1998), with $a_2/a_1 = 0.1$, $d/a_1 = 0.15$, $\mu_1/\mu_2 = 0.478/1.792$, $\nu_1 = 0.345$, $\nu_2 = 0.207$, and in plane strain condition

		K' at A	K' at B	K' at C	K' at D	$J\mu_2\approx$
$\vartheta = 60°$	Present	(1.7858, −0.0991)	(1.7662, 0.2661)	(1.4313, 0.36215)	(1.4773, −0.1173)	10^{-4}
	Chen, et al.	(1.786461, −0.09691)	(1.767574, 0.264866)	(1.430882, 0.362048)	(1.477131, −0.117351)	10^{-4}
$\vartheta = 120°$	Present	(1.7767, −0.0970)	(1.6194, 0.0823)	(0.4031, 0.3627)	(1.1223, 0.3543)	10^{-4}
	Chen, et al.	(1.777333, −0.09482)	(1.619560, 0.08076)	(0.403219, 0.362638)	(1.121970, 0.354160)	10^{-4}

and the J-integral consistency check (see Chen and Hasebe) is satisfied. The series terms used in this example was 30. From the above two examples, it is seen that the present method provides high accuracy and computational efficiency.

In the following examples, the moduli of the two materials are assumed as $E_2/E_1 = 10$, $\nu_1 = \nu_2 = 0.3$, and plane strain condition. If the loading normal to the interface is zero, and the loading parallel to the interface in material 2 is σ, the parallel loading in material 1 will then be $\Gamma\sigma$, with $\Gamma = 0.1$ for this case.

Fig. 4 shows the results of two cracks approaching the interface perpendicularly from the two materials under far loading parallel to the interface (crack geometric parameters are indicated in the figure). The energy release rates, G, increases as the two cracks approach the interface. This implies that the two cracks will tend to propagate towards the interface with the increasing far field load. For a single crack approaching the interface, if it approaches the interface from the stiffer material 2, G increases; whereas, if it approaches from the softer material 1, G decreases. This then indicates that the interface prevents the crack from the softer material to grow towards it. The energy release rate for a crack in the stiffer material 2, is higher than that for a crack in the softer material 1, when it is subjected to a load parallel to the interface (note the difference in coordinate scales).

Under loading parallel to the interface, the variation of the strain energy release rate as a crack in the stiffer material 2 approaches the interface and passes through it into the softer material 1, is depicted in Fig. 5. The results for the crossing interface crack are obtained by considering two cracks intersecting at the interface. When the crack approaches the interface, G increases and the rate of increase accelerates at

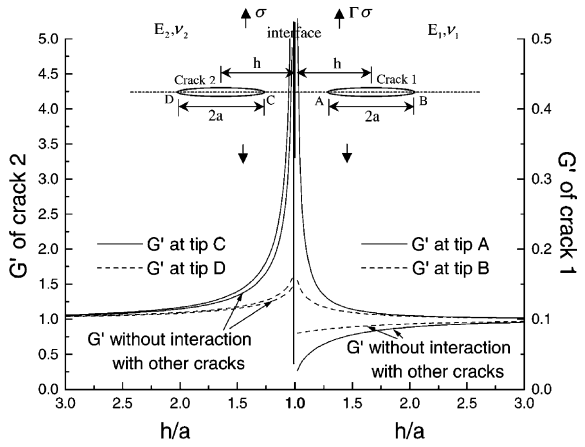

Fig. 4. The energy release rates (normalized by $\sigma^2\pi a(\kappa_2+1)/(8\mu_2)$), when two cracks approaches the interface perpendicularly from two planes, with $E_2/E_1 = 10$, $\nu_1 = \nu_2 = 0.3$.

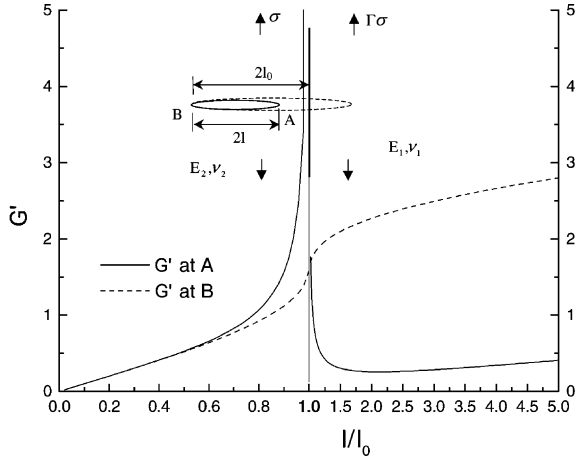

Fig. 5. The energy release rates (normalized by $\sigma^2\pi l_0(\kappa_2+1)/(8\mu_2)$), when a crack approaches and passes through the interface from material 2 (stiffer one).

the near interface tip A than that at the far tip B. This indicates that the crack will tend to grow towards the interface with increasing applied load. However, once the crack crosses the interface into the softer material, G at tip A decreases significantly, and become less than that at tip B. The implication of this is that the crack will not tend to grow further in the softer material, provided that the fracture toughness of the two materials are similar. Or more precisely, the crack will grow further in the softer material or propagate at the other tip B in the original material, depends on whether the energy release ratio at the two tips of the crack, $G(\mathrm{A})/G(\mathrm{B})$, is greater or less than the toughness ratio of the two materials, Γ_1/Γ_2. If $G(\mathrm{A})/G(\mathrm{B}) < \Gamma_1/\Gamma_2$, the crack will tend not to grow further in the softer material. Conversely, if the inequality is reversed, the crack will grow continuously at the tip B. After it has propagated some distance in material 1, G at tip A begins to increase gradually as the crack becomes longer. Note that G increases monotonically and gradually at tip B as the crack length increases.

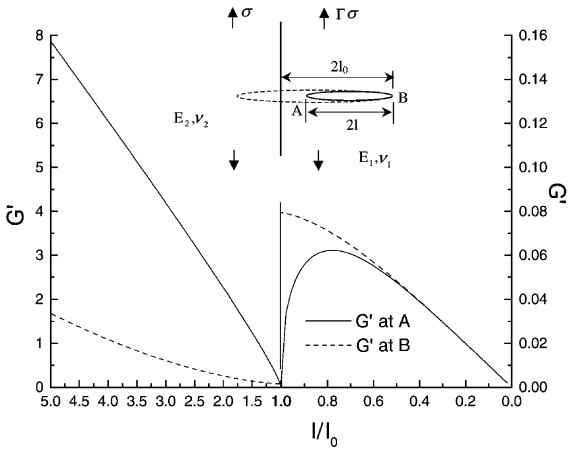

Fig. 6. The energy release rates (normalized by $\sigma^2\pi l_0(\kappa_2+1)/(8\mu_2)$), when a crack approaches and passes through the interface from material 1 (softer one).

The above example has practical significance. In composite laminates interleaves are inserted to increase a composite's fracture toughness and/or to arrest crack growth. The example indicates how to design such interleaves.

Fig. 6 shows a crack in the softer material 1, as it approaches the interface and passes through it into the stiffer material 2. When the crack approaches the interface, G decreases significantly at the near interface tip A. At the far tip B, G increases continuously, and becomes greater than that at the tip A. This implies that the interface tends to prevent the crack from growing towards the hard material. However, once the crack crosses the interface into the hard material 2, G at tip A increases significantly, and it exceeds that at tip B. This indicates that once the crack crosses the interface, the crack will tend to grow further in the stiffer material, assuming that the fracture toughness of the two materials are similar. Or more precisely, the crack will have a greater tendency to grow in the stiffer material, if $G(\mathrm{A})/G(\mathrm{B}) > \Gamma_2/\Gamma_1$. As the crack grows further, G also increases gradually at tip B, though it is much less than that at the tip A.

A crack surrounded by four stacked parallel cracks is shown in the insert in Figs. 7 and 8. This simulates the case of an infinite periodic array of cracks approaching the interface from the stiffer material 2 (Fig. 7) and softer material 1 (Fig. 8). The energy release rates of the central crack as it approaches the interface are shown in Figs. 7 and 8, respectively. When the distance h of stacked cracks is very large, the interacting effect among cracks is small, and the effect of interface on the crack has been presented before in Figs. 5 and 6. The stacked cracks display shielding effect (decreasing the energy release rate), and this effect increases as the crack distance h decreases. As the distance h decreases to a certain limit, such as $h < 0.11_0$, the energy release rate of the central crack tends to zero, which implies that densely stacked cracks will prevent new cracks from forming, and there will exist a saturation state of crack density.

The results predicted in Fig. 8 are in agreement with experimental observations reported by Wolodko et al. (1999). Digital images of parallel cracks in a cross-ply laminate $[0_2/90_3]_S$ glass fiber/epoxy matrix specimens were captured at predetermined loading levels in these experiments. Fig. 9 shows an experimentally captured map of transverse crack evolution at four levels of increasing applied strain in the longitudinal direction (0°). It is noted that the crack density tends towards a saturated level as the distance between the transverse cracks decreases. Upon further load increase, there will be a change in failure mechanism as the 0° fibres will carry the additional load.

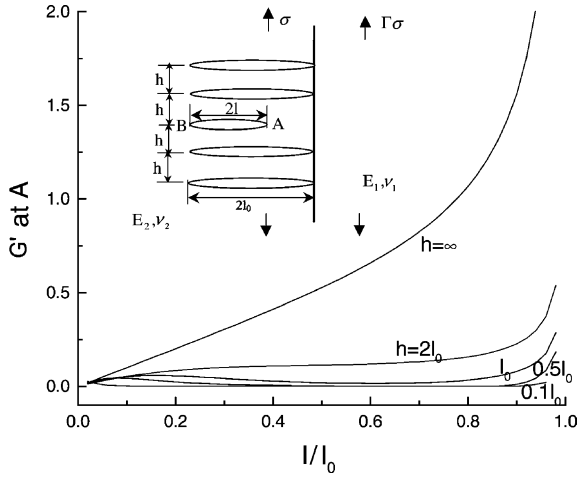

Fig. 7. The energy release rates (normalized by $\sigma^2\pi l_0(\kappa_2+1)/(8\mu_2)$), when a crack surrounded by four stacked cracks approaches the interface from material 2 (stiffer one).

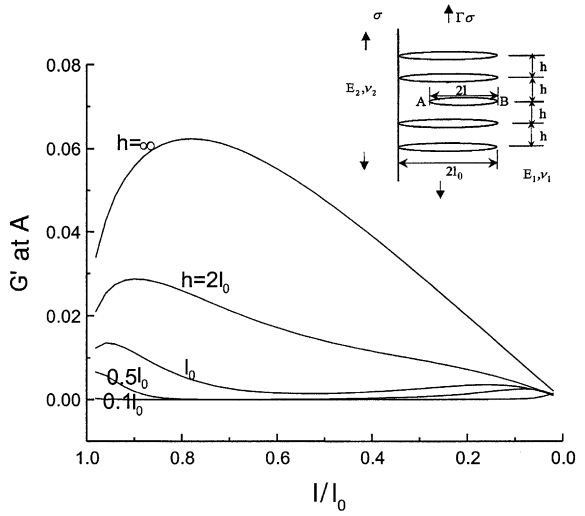

Fig. 8. The energy release rates (normalized by $\sigma^2\pi l_0(\kappa_2+1)/(8\mu_2)$), when a crack surrounded by four stacked cracks approaches the interface from material 1 (softer one).

In the following examples, the remote tensional loading is perpendicular to the interface and $\sigma_y^\infty=\sigma$, the loading parallel to the interface in material 2 is zero, i.e. $\sigma_{x2}^\infty=0$, and σ_{x1}^∞, the remote parallel loading in material 1 is obtained from Eq. (1),

$$\sigma_{x1}^\infty=\frac{1}{1+\kappa_1}\left[3-\kappa_1-\frac{\mu_1}{\mu_2}(3-\kappa_2)\right]\sigma_y^\infty=\lambda\sigma_y^\infty \tag{17}$$

where the symbols have already been defined following Eq. (1).

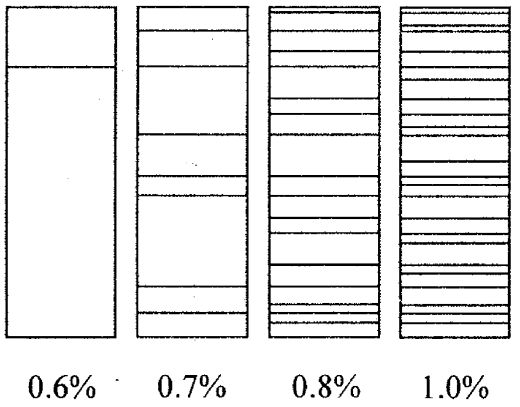

Fig. 9. Experimental observation of transverse cracks at various applied strain levels in a $[0_2/90_3]_S$ glass fiber reinforced epoxy resin composite laminate.

Fig. 10 shows the results of an interface crack interacting with one or two nearby cracks under remote tension loading. In Fig. 10(a) the non-interfacial cracks are parallel to the interface while those in Fig. 10(b) are inclined 30°. When the interface crack (called main crack here) is under the surrounding crack(s) ($l < 1.5a$), the energy release rate at the main crack tip A becomes less than that without interaction with other cracks. This indicates that the main crack is shielded by the stacked cracks. When the surrounding crack(s) is further away from the stacked arrangement ($l > 1.5a$), the energy release rate of the main crack increases. This shows that the main crack is now anti-shielded. It is also noted that a crack in the softer material 1, has a more interaction effect on the interface crack than a crack with a similar position but in the stiffer material 2.

Fig. 11 depicts an interface crack interacting with a parallel sub-crack subjected to a load normal to the interface and cracks. When the position of the sub-crack is made to approach the interface, we note an increase in the interaction effect of the cracks. It is also noted that the greatest amplified value is reached when the sub-crack is not at the interface position but slightly away from the interface in the softer material 1. The energy release rate for the sub-crack in the softer material 1, is greater than that in a similar position but in the stiffer material 2. Without interaction with other cracks, the energy release rate for the sub-crack will decrease gradually, as the position of sub-crack changes from a far away location in material 1, to the interface, and again away from the interface in material 2.

4. Discussion and conclusion

A simple and unified method is presented to treat the interaction problem of cracks, dislocations, and interface in two bonded different materials. The multiple cracks and dislocations can be arbitrarily distributed, including interfacial ones, in a bonded half planes. Although the present analysis is derived for distributed *non-intersecting* cracks, it can also be applied to intersected cracks, such as kinked and branched cracks, by invoking the single-valued condition of displacements to intersected cracks. In the present paper, the existing dislocations are not emitted from any special crack tip. The interacting fields for dislocations emitted from a crack are different from those originated elsewhere (see Zhang and Li (1991, 1992)), however, they can also be analyzed by the present method. When the moduli of the bonded materials are the same, or the moduli of one material become zero, the bonded bi-material problem reduces to a

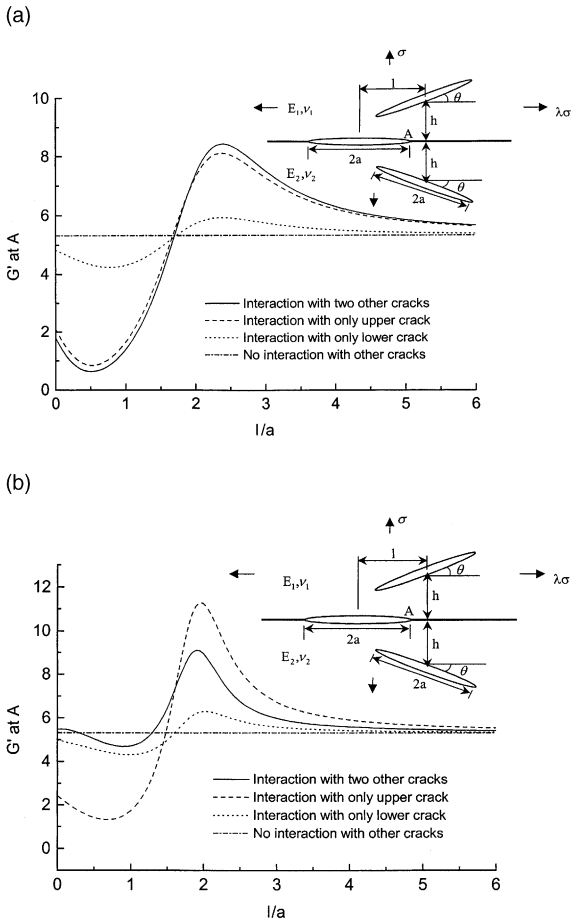

Fig. 10. The energy release rate (normalized by $\sigma^2\pi a(\kappa_2+1)/(8\mu_2)$) of an interface crack, when it interacts with two other cracks with angles θ: (a) $\theta = 0°$, and (b) $\theta = 30°$.

homogenous one and a half-plane one, respectively. Numerical examples show that the method yields high numerical accuracy and computational efficiency. Several examples are given to show certain interaction effects which are also of practical interest. The following conclusions are drawn based on these case study examples:

The energy release rate of a crack in the softer material is greater than that in the stiffer material, when the bi-material plate is subjected to far field loads normal to the interface, and vice versa when it is subjected to far field loads parallel to the interface.

A crack approaching an interface from a stiffer material at first tends to grow towards the interface. However, once the crack crosses the interface, the crack may not grow further in the softer material, if the fracture toughness of the two materials is similar. Conversely, when a crack approaches an interface from a softer material, it tends to slow down, however, once it has crossed the interface, it will continue to propagate into the stiffer material.

If a crack is surrounded by some nearby stack arranged cracks, the crack will usually be shielded. Experimental evidence is provided to support the above prediction. An amplifying effect may occur, however, if the surrounding cracks are moved a certain distance away parallel to the interface.

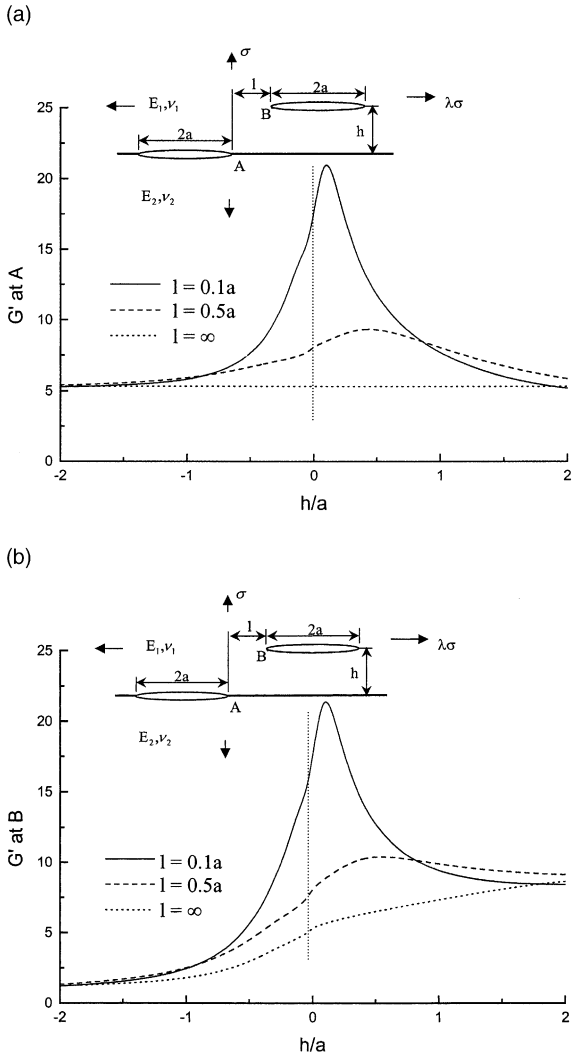

Fig. 11. The energy release rates (normalized by $\sigma^2\pi a(\kappa_2+1)/(8\mu_2)$) of an interface crack interacting with another parallel crack: (a) at the tip A of the interface crack, and (b) at the tip B of the other parallel crack.

When an interface crack interacts with a parallel sub-crack, the amplified interaction effect occurs when the two cracks are nearly in a line, and the greatest amplified effect is observed when the sub-interface crack is near but a little away from the interface in the softer material.

Acknowledgements

This investigation is part of a program concerned with the damage development and crack propagation in polymeric composites. The research is support, in part, by the Natural Sciences and Engineering Research Council of Canada (NSERC), through grants to F.E. & Z.X. X.H. is grateful to the support from Chinese Academy of Sciences to scholars returning from abroad.

References

Burton Jr., J.K., Phoenix, S.L., 2000. Superposition method for calculating singular stress fields at kinks, branches and tips in multiple crack arrays. International Journal of Fracture 102, 99–139.

Chen, Y.H., Hasebe, N., 1998. A consistency check for strongly interacting multiple crack problems in isotropic, bimaterial and orthotropic bodies. International Journal of Fracture 89, 333–353.

Chen, Y.Z., 1986. Multiple crack problems for two bonded half planes in plane and antiplane elasticity. Engineering Fracture Mechanics 25, 1–9.

Chen, Y.Z., 1995. A survey of new integral equations in plane elasticity crack problem. Engineering Fracture Mechanics 51, 97–134.

Erdogan, F., Gupta, G.D., Cook, T.S., 1973. Numerical solution of singular integral equations. In: Sih, G.C. (Ed.), Mechanics of Fracture, vol. 1. Noordhoff, Groningen, pp. 368–425.

Goree, J.G., Venezia, W.A., 1977. Bonded elastic half-planes with an interface crack and a perpendicular intersecting crack that extends into the adjacent material. International Journal of Engineering Science 15, 1–17.

Gross, D., 1982. Stress intensity factors of systems of cracks. Ingenieur Archiv 51, 301–310.

Hills, D.A., Kelly, P.A., Dai, D.N., Korsunsky, A.M., 1996. Solution of Crack Problems: The Distributed Dislocation Technique. Kluwer Academic Publishes, Dordrecht, The Netherland.

Hu, K.X., Chandra, A., Huang, Y., 1994. On crack, rigid-line fiber, and interface interactions. Mechanics of Materials 19, 15–28.

Isida, M., Noguchi, H., 1993. Arbitrarily array of cracks in bonded half planes subjected to various loadings. Engineering Fracture Mechanics 46, 365–380.

Isida, M., Noguchi, H., 1994. Distributed cracks and kinked cracks in bonded dissimilar half planes with an interface crack. International Journal of Fracture 66, 313–337.

Kachanov, M., 1994. Elastic solids with many cracks and related problems. In: Hutchinson, J.W., Wu, T.Y. (Eds.), Advances in Applied Mechanics, vol. 30. Academic Press, New York.

Murakami, Y. et al., 1987. Stress Intensity Factors Handbook, vol. 1. Pergamon Press, Oxford.

Muskhelishvili, N.I., 1953. Some Basic Problems of the Mathematical Theory of Elasticity. Noordhoff, Groningen, Holland.

Otsu, T., Wang, W.X., Takao, Y, 1999. Asymmetrical cracks parallel to an interface between dissimilar materials. International Journal of Fracture 96, 75–100.

Suo, Z., 1989. Singularities interacting with interfaces and cracks. International Journal of Solids and Structures 25, 1133–1142.

Wolodko, J.D., Hoover, J.W., Ellyin, F., 1999. Detection of transverse cracks in GFRP composites using digital image processing. In: Ellyin, F., Proven, J.W. (Eds.), Progress in Mechanical Behaviour of Materials, vol. 2. ICM8, Victoria, Canada, pp. 483–487.

Zhang, T.Y., Li, J.C.M., 1991. Image forces and shielding effects of an edge dislocation near a finite length crack. Acta Metallurgica et Materialia 39, 2739–2744.

Zhang, T.Y., Li, J.C.M., 1992. Interaction of an edge dislocation with an interfacial crack. Journal of Applied Physics 72, 2215–2226.

Zhao, L.G., Chen, Y.H., 1996. Interaction between an interface crack and a parallel subinterface crack. International Journal of Fracture 76, 279–291.